Collective enhancement in nuclear level density of ^{72}Ga and ^{71}Ga from γ-gated proton spectra

Rajkumar Santra,[1,*] Balaram Dey,[2] Subinit Roy,[3] R. Palit,[1] Md. S. R. Laskar,[1] H. Pai,[4] S. Rajbanshi,[5] Sajad Ali,[6] Saikat Bhattacharjee,[3] F. S. Babra,[1] Anjali Mukherjee,[3] S. Jadhav,[1] Balaji S. Naidu,[1] Abraham T. Vazhappilly,[1] and Sanjoy Pal[1]

[1]*Department of Nuclear and Atomic Physics, Tata Institute of Fundamental Research, Mumbai 400005, India*
[2]*Department of Physics, Bankura University, Bankura 722155, India*
[3]*Nuclear Physics Division, Saha Institute of Nuclear Physics, Kolkata 700064, India*
[4]*Extreme Light Infrastructure - Nuclear Physics, Bucharest-Magurele 077125, Romania*
[5]*Department of Physics, Presidency University, Kolkata 700073, India*
[6]*Government General Degree College at Pedong, Kalimpong 734311, India*

(Received 25 April 2023; accepted 7 June 2023; published 26 June 2023)

The γ-gated proton spectra measured in the reactions ^{64}Ni(^{9}Be, p2n)^{70}Ga and ^{64}Ni(^{9}Be, pn)^{71}Ga, have been utilized to probe the collective enhancement in nuclear level density (NLD) of two oblate deformed nuclei ^{71}Ga and ^{72}Ga. It is seen that the γ-gated proton spectrum are reasonably explained by using the large value of the inverse level density parameter ($k = 11.2$ MeV) in the NLD prescription of the Fermi gas model. The large value of k indicates rotational enhancement, which is consistent with the earlier results in other mass regions. Furthermore, a rotational enhancement factor has been included in the NLD and used in the statistical model calculation keeping the systematic value of $= 8.6$ MeV. It explains the γ-gated proton spectrum nicely, which indicates the presence of collective enhancement in the NLD. The extracted enhancement factors are found to be 8.0+/−2.0 and 5.5+/−1.0 and vanish at around 15, 18 MeV excitation energies for ^{71}Ga, ^{72}Ga, respectively. Present observations are consistent with the previous results obtained by Pandit *et al.* [Phys. Rev. C **97**, 041301(R) (2018)] and Mohanto *et al.* [Phys. Rev. C **100**, 011602(R) (2019)].

DOI: 10.1103/PhysRevC.107.064611

I. INTRODUCTION

Atomic nucleus is a quantum many-body system, which exhibits both single-particle as well as collective nature in its excitation spectra [1]. The density of these quantum levels increases rapidly with the increase in excitation energy and soon becomes extremely large. Consequently, the concept of nuclear level density (NLD) [2], defined as the number of excited levels per unit of excitation energy for a nucleus, is required for the description of nuclear reactions and in many applied areas. The NLD contains internal structure of nuclei such as its mode of excitation such as single-particle mode of excitation, collective mode of excitation, etc. It was theoretically predicted [3–6] that due to the inclusion of collective degrees of freedom (such as rotation and vibration) there should be an enhancement in NLD over its single-particle value, which would subsequently get fade out at higher excitation. From microscopic study [4], it was predicted that for finite ground-state deformation of nuclei the rotational enhancement factor (K_{rot}) is ≈100 and melt around 50 MeV excitation energy. Microscopically, the results of the Monte Carlo shell model calculation [5] indicate that rotational enhancement factor is ≈10 and fade out at energy around 18–30 MeV.

The first experimental evidence of collective enhancement in NLD was probed indirectly by Junghans *et al.* [7] by measuring the fragments yield distribution for even-Z isotopes from osmium to uranium. There was no evidence of collective enhancement in measurement of α evaporation from CN ^{178}Hf over the excitation energy range 54–124 MeV [8]. Most recently, the collective enhancement in NLD for the mass region $A \geqslant 150$ was obtained from fusion evaporation measurement [9–13]. However, very few experimental attempts have been made to estimate the rotational enhancement factor and its fadeout energy [11–13]. The rotational enhancement factor for ^{187}Os obtained from neutron evaporation spectra by Mohanto *et al.* [13] was found to be 6 and die out at around 25 MeV excitation energy. On the other hand, Pandit *et al.* [11] showed that the rotational enhancement factor obtained from angular momentum gated proton, neutron, and giant dipole resonance (GDR) γ spectra are very similar (≈10) and die out at around 15 MeV excitation energy for ^{168}Tm, ^{169}Tm, ^{168}Er, ^{185}Re, ^{184}Re, ^{184}W nuclei. Therefore, it is still a very confusing and intriguing topic to have a clear understanding of collective enhancement and its fade out, and demands further systematic investigation.

The primary goal of the present work is to investigate the collective enhancement in the NLDs of ground-state oblate deformed nuclei ^{72}Ga and ^{71}Ga by using the particle-γ coincidence technique. Very recently, we adopted a new approach to select the evaporated particles only from compound nu-

*rajkumarsantra2013@gmail.com

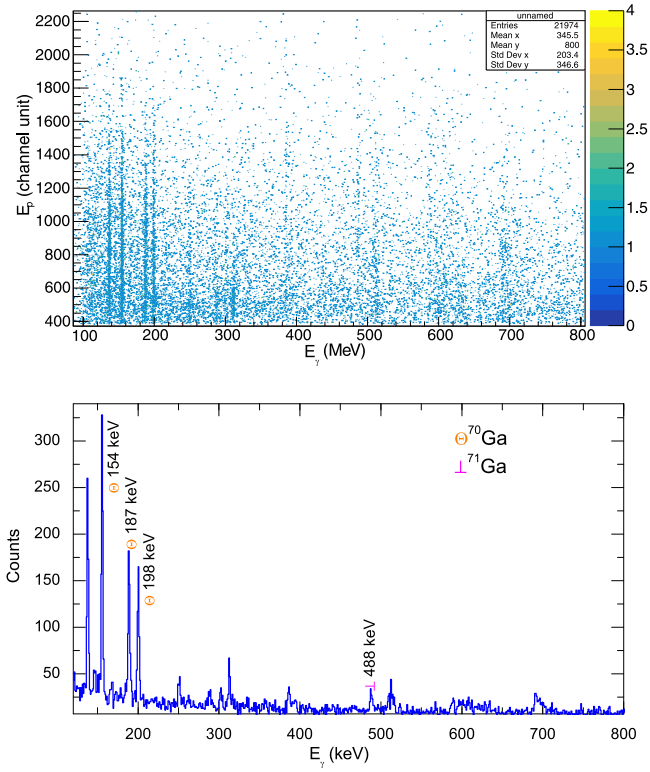

FIG. 1. (Top) p-γ coincidence matrix extracted from raw particle-γ matrix. (Bottom) Projected γ energy spectrum. Symbols with γ energy indicate γ lines of different residual nuclei associated with proton emitting channels.

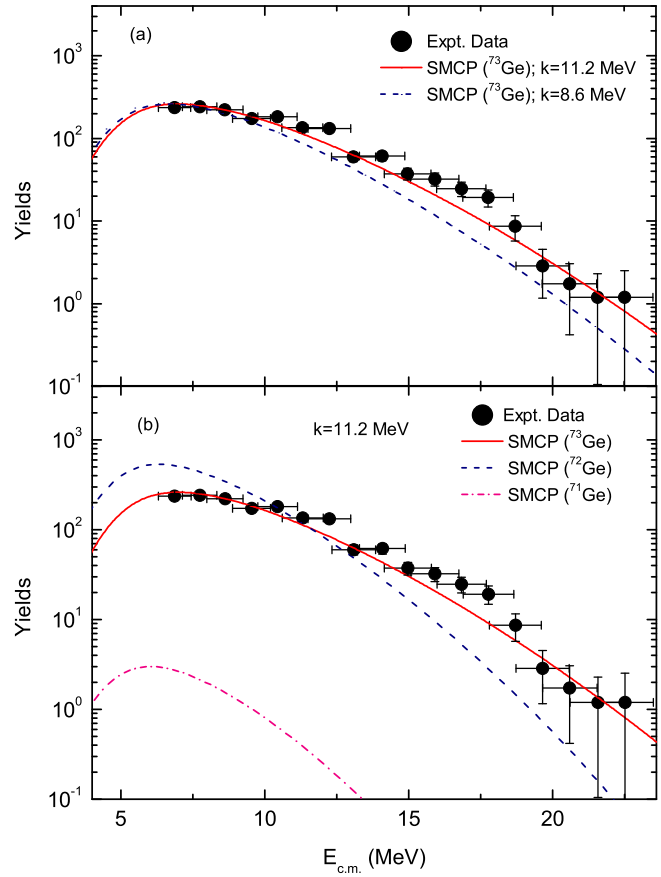

FIG. 2. Filled symbols represent the experimental γ-gated proton spectrum. Lines represent the statistical model calculated proton (SMCP) spectrum. (Top) Red solid and blue dashed lines represent SMCP spectrum considering first chance proton emission from CN, with $k = 11.2$ MeV and $k = 8.6$ MeV, respectively. (Bottom) Red continuous, blue dashed, and pink dash-dotted lines represent SMCP spectrum considering first. second, and third chance proton emission from CN, respectively, with $k = 11.2$ MeV.

clear reactions by using the γ-gated particle spectra [14]. The same approach, as discussed in Ref. [14] has been used in the present work. In this work, we have measured the γ-gated evaporated protons coming from the reactions ^{64}Ni(^{9}Be, p2nγ)^{70}Ga and ^{64}Ni(^{9}Be, pnγ)^{71}Ga. Particle-γ coincidence has been performed to eliminate the events from target contamination and preequilibrium emission. The γ-gated proton spectra have been utilized to obtain the level densities of residual nuclei.

The ^{9}Be beam of 30 MeV energy with an average current of 5 nA from BARC-TIFR Pelletron Linac Facility, Mumbai, was used to bombard a self-supporting ^{64}Ni target of thickness 500 μg/cm^2, populating the ^{73}Ge compound nucleus (CN). The outgoing protons were detected by using CsI(Tl) detectors with the angle of coverage from 22°–67°. The 14 Compton-suppressed Clover detectors were used to detect the deexciting discrete γ-rays coming from the residual nuclei. XIA-LLC-based digital data acquisition system was used to store the data in list mode. Tantalum foil of thickness 30 mg/cm^2 was used to stop the elastically scattered events from entering the detectors. The proton spectrum is calibrated using ^{229}Th source with pulse height defect correction based on light output vs. energy data of CsI(Tl) in Ref. [15]. Multiparameter time-stamped based coincidence search program (MARCOS) [16] was used to construct the p-γ matrix as shown in Fig. 1. From this matrix, proton yield spectra were extracted gated by characteristic 154.9 ($5^- \rightarrow 4^-$), 187.6 ($4^- \rightarrow 2^-$), 198 keV γ rays from the residual ^{70}Ga nucleus and 488 keV γ ray from ^{71}Ga nucleus [17] by p2n and pn evaporations from ^{73}Ge compound nucleus. Finally, the γ-gated proton spectra are added after efficiency correction ($Y_{\text{total}} = \frac{Y_{154}}{\epsilon_{154}} + \frac{Y_{187}}{\epsilon_{187}} + \frac{Y_{198}}{\epsilon_{198}} + \frac{Y_{488}}{\epsilon_{488}}$) to visualize the shape of the final proton spectrum with higher statistics as shown in Fig. 2. The quantities, ϵ_i and Y_i, are the detection efficiency of ith γ ray and the yield of proton that are in coincidence with the ith γ ray.

In order to investigate the NLD of residual nuclei, the γ-gated proton spectrum has been compared with the statistical model calculations using the code CASCADE [18] with the Fermi-gas (FG) model of NLD given by

$$\rho(E^*, J) = \frac{2J+1}{12\theta^{3/2}}\sqrt{a}\frac{\exp(2\sqrt{aU})}{U^2}, \quad (1)$$

where, $U = E^* - \frac{J(J+1)}{\theta} - S_p - \Delta P$, E^*, and J are the initial excitation energy and the angular momentum of the nucleus, respectively, $\theta = \frac{2I_{\text{eff}}}{\hbar^2}$, with I_{eff}, S_p, and ΔP being the effective rigid-body moment of inertia, the proton separation energy,

and the pairing energy, respectively. The quantity a in Eq. (1) is the level density parameter. Ignatyuk prescription [19] of level density parameter a, which takes into account the shell effect as a function of excitation energy is adopted and it is expressed as

$$a = \tilde{a}\left[1 + \frac{\delta S}{U}[1 - \exp(-\gamma U)]\right], \tag{2}$$

where asymptotic level density parameter $\tilde{a} = \mathrm{A}/k$ and k is the inverse density parameter. δS is the ground-state shell correction defined as the difference of the experimental and theoretical (liquid drop) masses. The inverse of γ in the exponent of Eq. (2), given by $\gamma^{-1} = \frac{0.4A^{4/3}}{\tilde{a}}$ is the rate at which the shell effect is damped with the increase in excitation energy. The optical model potential parameters for proton transmission coefficient are taken from Ref. [20]. The moment of inertia of the CN is taken as $I_{\mathrm{eff}} = I_0(1 + \delta_1 J^2 + \delta_2 J^4)$, where $I_0(=\frac{2}{5}MA^{5/3}r_0^2)$ is the moment of inertia of a spherical nucleus, δ_1 ($=1.0 \times 10^{-4}$) and δ_2 ($=2.0 \times 10^{-6}$) are the deformability parameters, $\mathrm{r}_0 = 1.25$ fm is the radius parameter and J is the total spin of the nucleus. It is seen that the choice of proton optical potential has negligible effect on the slope of the spectrum. The deformability parameters have also negligible effect on slope (δ_1 change from 10^{-6}–10^{-4} and δ_2 change from 10^{-8}–10^{-6}). The slope of the spectrum mainly depends on the inverse level density parameter k, which is generally varied to explain the evaporated particle spectrum by using χ^2 minimization technique.

The γ-gated proton spectrum along with the statistical model calculations is shown in Fig. 2. It is observed that the systematic value of k (8.6 MeV) is unable to explain the experimental data above 10 MeV as shown in Fig. 2(a). Indeed, a large value of k (11.2 MeV) is required to explain the experimental data considering the emission of first chance protons from CN as shown in Fig. 2(a) and the value of the reduced $\chi^2(\frac{\chi^2}{N})$ for the fit is 4.51. This observation is consistent with the previous results obtained in Refs. [10,11]. The ground-state quadrupole deformations of ^{71}Ga and ^{72}Ga are -0.207 and -0.215, respectively, as reported by Moller *et al.* [21]. Moreover, rotational bands have also been observed up to the 4.2 MeV excitation energy in ^{71}Ga [22]. One can also expect a rotational band structure at high spin in ^{72}Ga. So the collective enhancement due to ground-state deformation of the residual nucleus could be the possible indication for this large k value. On the other hand, as the evaporated proton spectrum is gated with the γ-rays of ^{70}Ga and ^{71}Ga residual nuclei, it could also contain the contributions of protons coming out after one or two neutrons (1n or 2n) emitted from the CN. Therefore, a statistical model calculation has been carried out by using $k = 11.2$ MeV to obtain the proton spectrum after 1n and 2n emissions and compared with the experimental data as shown in Fig. 2(b). It should be mentioned that the same normalization has been used in each case (protons from the first chance, protons after 1n emission, and protons after 2n emission) while comparing with the experimental data. It is seen that there could have been some contributions of protons after 1n emission. However, the proton after 2n emission is negligibly small as shown in Fig. 2(b).

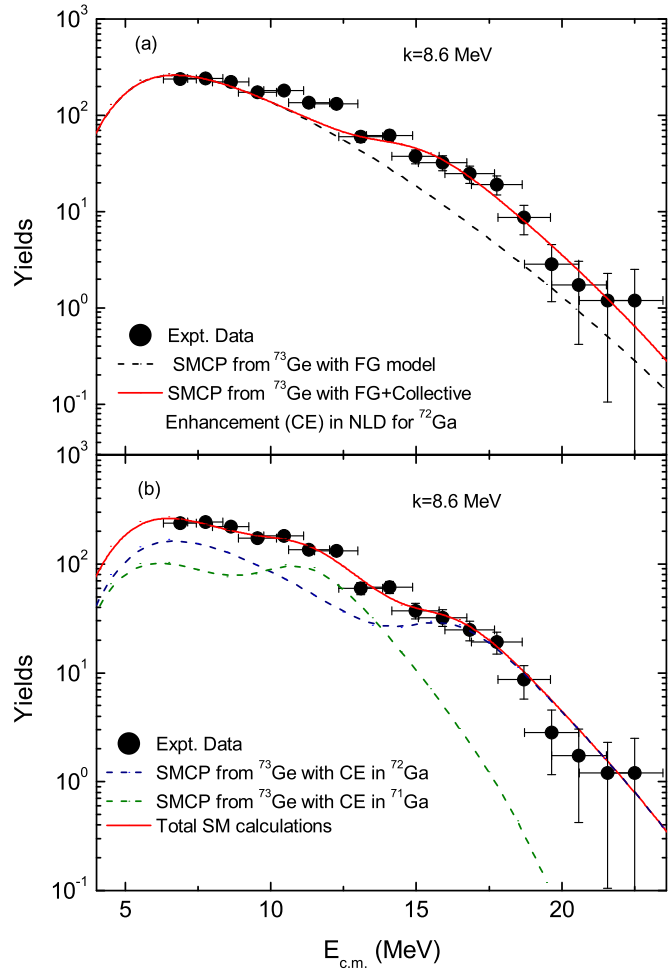

FIG. 3. Filled symbols represent the γ-gated proton spectrum. Lines represent the statistical model calculated proton (SMCP) spectrum. (Top) Red continuous line represents SMCP with $k = 8.6$ MeV considering first chance proton emission from CN ^{73}Ge and including collective enhancement (CE) factor in NLD of ^{72}Ga residual nucleus. (Bottom) Purple dashed line represents SMCP with $k = 8.6$ MeV considering first chance proton emission from CN ^{73}Ge and including collective enhancement factor in NLD of ^{72}Ga residual nucleus. Pink dashed line represents SMCP with $k = 8.6$ MeV considering second chance proton emission from CN ^{73}Ge and including collective enhancement factor in NLD of ^{71}Ga residual nucleus. Red continuous line represents the total spectrum with weightage factor as $\mathrm{Y_{total}} = \mathrm{Y(first\ chance)} + 0.3\times\mathrm{Y}(2^{\mathrm{nd}}\ \mathrm{chance})$. In figure CE means collective enhancement.

A large value of $k = 11.2$ MeV from the statistical model analysis with FG model for NLD and the bumps around the center-of-mass energies of 12 MeV and 15 MeV, could be a possible reason for the existence of collective enhancement in NLD due to the deformation of the residual nuclei. In a subsequent analysis, the γ-gated proton spectrum has been compared with the statistical model calculated proton (SMCP) spectrum by including the collective enhancement factor in NLD of ^{72}Ga residual nucleus as shown in Fig. 3. The model calculation has been carried out by considering first chance proton emission with the systematic value of $k = 8.6$ MeV

(which best explains the low-energy part of the proton spectra below 10 MeV) and a rotational enhancement factor ($K_{\rm rot}$) has been included as $\rho = \rho_{\rm int} K_{\rm rot}$, where $\rho_{\rm int}$ is intrinsic level density. The factor $K_{\rm rot}$ is introduced with the intrinsic single-particle level density to consider the contribution of rotational enhancement factor in the NLD. Microscopic shell model studies [10] have predicted that for nuclei with finite ground-state deformation, rotational levels collectively causes large enhancement of NLD ($K_{\rm rot} \approx 100$). With increasing excitation energy, the deformation effect gradually dies down due to the intrinsic motion. Therefore, the deformed shape of the residual nucleus changes into spherical shape and rotational levels die out. Due to this shape transition, fade out of collective enhancement in NLD is observed after a certain excitation energy. The energy-dependent Fermi function made by Hansen *et al.* [4] has been used in the rotational enhancement factor given as

$$K_{\rm rot} = (\sigma_\perp^2 - 1) \times f(E) + 1 \tag{3}$$

$$f(E) = \frac{1}{1 + \exp\left(\frac{E - E_{\rm cr}}{d_{\rm cr}}\right)}. \tag{4}$$

The spin cutoff parameter, $\sigma_\perp^2$ is replaced by λT, where $T[= \sqrt{(U/a)}]$ is nuclear temperature and λ is treated as the magnitude of the enhancement parameter. The parameters λ, $E_{\rm cr}$, and $d_{\rm cr}$ are generally varied to explain the experimental data. It is observed that the experimental data below 10 MeV and above 13 MeV are nicely described by the result of the statistical model calculation considering the first chance protons and including the rotational enhancement in NLD of ^{72}Ga, as shown in Fig. 3(a). However, the experimental data in between 10–13 MeV center-of-mass energy cannot be explained. This conjecture is the presence of protons from second chance emission in that energy domain. Therefore, the proton spectrum has also been calculated considering the level density and including the rotational enhancement factor of ^{71}Ga residual nucleus and shown in Fig. 3(b). Finally, the first and second chance statistical model calculated proton (SMCP) spectra are added with weightage obtaining the total yield as $Y_{\rm total} = Y$ (first chance) $+ w \times Y$ (second chance), which nicely explains the γ-gated proton spectrum as shown in Fig. 3(b). A χ^2 minimization procedure, with parameters from two rotational enhancement factors corresponding to the NLDs of residual nuclei ^{72}Ga and ^{71}Ga and the weight factor w in the total yield, has been carried out to fit the experimental spectrum.

The best fit parameters of the rotational enhancement factors, the weight factor (w), and the corresponding χ^2 per degrees of freedom are listed in Table I. The fit including the enhancements in the NLDs of ^{71,72}Ga isotopes explain the particle spectrum with significant improvement in reduced χ^2 value.

In Fig. 4, the present NLDs of ^{72}Ga and ^{71}Ga (used in CASCADE calculation) have been plotted as a function of excitation energy and also compared with the cumulative level density computed from the levels given in the RIPL-3 [23] at low excitation energy. The NLD of ^{72}Ga is normalized with the experimental NLD at S_n obtained from neutron resonance spacing [24]. As the experimental NLD of ^{71}Ga at S_n (from neutron resonance studies) is not available, the present NLD of ^{71}Ga is normalized with RIPL-3 [23] data at 1.9 MeV excitation energy. The constant temperature (CT) model, which is known to best describe the level densities in the low excitation energy domain up to the particle threshold energy, is represented by a solid curve. The CT model level density is given as $\rho_{\rm CT} = \frac{1}{T} e^{(E-E_0)/T}$, where T and E_0 as free parameters. It should be mentioned that the systematic values of CT model parameters [24] obtained from the fitting of the NLD data from RIPL-3 and the data at the neutron separation energy (S_n) [24] are used while comparing with the level density of ^{72}Ga and ^{71}Ga from the present work. The important aspects of the comparisons in Fig. 4 should be emphasized here. It is

TABLE I. Summary of the best fit parameters of the rotational enhancement factor used in NLD of SMCP calculations and the weight factor.

Nucleus	λ (MeV^{-1})	$E_{\rm cr}$ (MeV)	$d_{\rm cr}$ (MeV)	w	$\frac{\chi^2}{N}$
^{72}Ga	6.0 ± 0.5	14.3 ± 0.5	0.7 ± 0.1	0.3	1.99
^{71}Ga	10.0 ± 0.5	11 ± 0.6	0.7 ± 0.12		

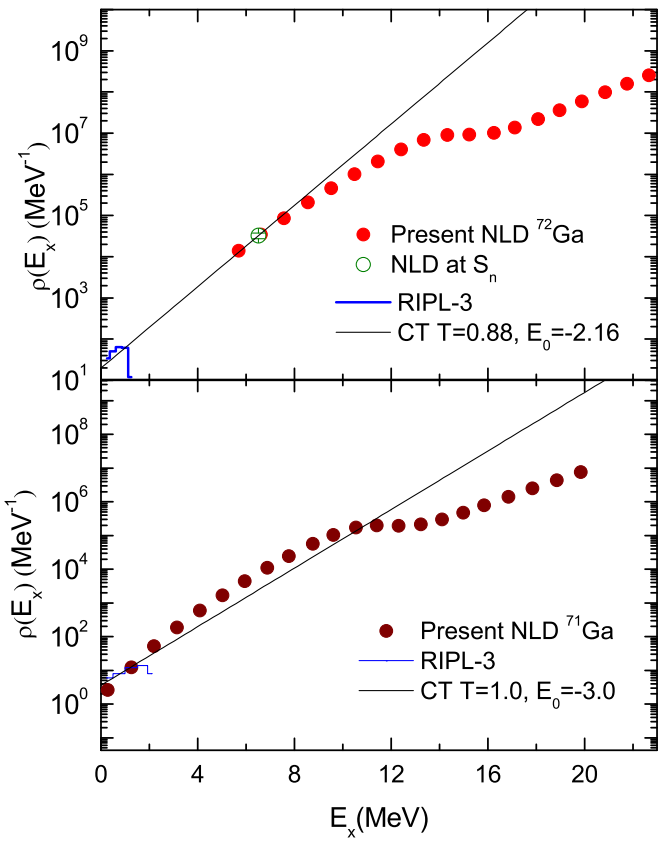

FIG. 4. The enhanced nuclear level densities as a function of excitation energy are shown as used in the CASCADE. Histogram represents the cumulative level density computed from the known levels given in the RIPL-3 [23].

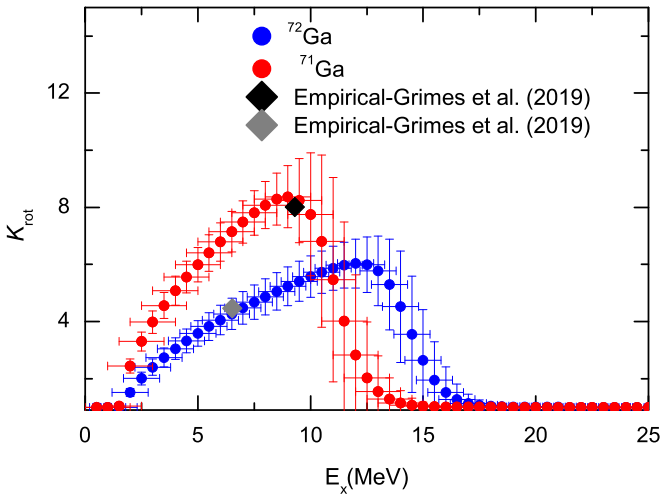

FIG. 5. The rotational enhancement factor of ^{72}Ga and ^{71}Ga are plotted as a function of excitation energy and results compared with Grimes [25] empirical formula at S_n.

seen that the extracted density that includes the enhancement effect follows the trend of the CT model prediction locally around the normalization point at S_n for ^{72}Ga. However, for ^{71}Ga the present NLD is almost close to the CT model prediction up to 11 MeV excitation energy and above 11 MeV as the collective enhancement effect wanes, the NLD from the present work deviates from CT model prediction.

The rotational enhancement factors (K_{rot}) for ^{72}Ga and ^{71}Ga are also extracted as a function of excitation energy as shown in Fig. 5. The K_{rot} at S_n is compared with the values estimated from Grimes [25] empirical formula at S_n and found to be very close with present results for ^{71}Ga, ^{72}Ga plotted in Fig. 5. The observation of K_{rot} fadeout at energies of 15 and 18 MeV for ^{71}Ga and ^{72}Ga, respectively, are consistent with earlier results [11,13].

In summary, the measured γ-gated proton spectrum is predominantly from the compound nuclear process, which is ensured by the coincidence measurement with selected γ rays from the residues of p2n and pn channels following the ^{9}Be + ^{64}Ni reaction. The γ-gated proton spectrum has been utilized to obtain the level densities of residual nuclei (^{72}Ga and ^{71}Ga). It is observed that collective enhancement factors due to the deformation of residual nuclei are included in the NLD prescription of the Fermi-gas (FG) model to explain the experimental γ-gated proton spectrum. The extracted rotational enhancement factor for ^{71}Ga and ^{72}Ga was 8.0+/−2.0 and 5.5+/−1.0, and the fadeout of the enhancement occurred around 15 MeV and 18 MeV excitation for the two deformed isotopes having very similar ground-state deformations.

ACKNOWLEDGMENTS

We would like to thank Dr. D. Pandit, VECC for his help and advice in this project. Authors thank the BARC-TIFR PLF staff for uninterrupted, steady beam during the experiment. This work is supported by the Department of Atomic Energy, Government of India (Project Identification No. RTI 4002), and the Department of Science and Technology, Government of India (Grant No. IR/S2/PF-03/2003-II).

[1] A. Bohr and B. R. Mottelson, *Nuclear Structure* (Benjamin, New York, 1969), Vol. 1.
[2] H. A. Bethe, Phys. Rev. **50**, 332 (1936); Rev. Mod. Phys. **9**, 69 (1937).
[3] A. V. Ignatyuk, K. K. Istekov, and G. N. Smirenkin, Sov. J. Nucl. Phys. **29**, 450 (1979).
[4] G. Hansen and A. S. Jensen, Nucl. Phys. A **406**, 236 (1983).
[5] C. Özen, Y. Alhassid, and H. Nakada, Phys. Rev. Lett. **110**, 042502 (2013).
[6] S. Karampagia and V. Zelevinsky, Phys. Rev. C **94**, 014321 (2016).
[7] A. R. Junghans *et al.*, Nucl. Phys. A **629**, 635 (1998).
[8] S. Komarov, R. J. Charity, C. J. Chiara, W. Reviol, D. G. Sarantites, L. G. Sobotka, A. L. Caraley, M. P. Carpenter, and D. Seweryniak, Phys. Rev. C **75**, 064611 (2007).
[9] P. Roy *et al.*, Phys. Rev. C **88**, 031601(R) (2013).
[10] K. Banerjee *et al.*, Phys. Lett. B **772**, 105 (2017).
[11] D. Pandit *et al.*, Phys. Rev. C **97**, 041301(R) (2018).
[12] D. Pandit *et al.*, Phys. Lett. B **816**, 136173 (2021).
[13] G. Mohanto *et al.*, Phys. Rev. C **100**, 011602(R) (2019).
[14] R. Santra *et al.*, Phys. Lett. B **806**, 135487 (2020).
[15] D. Dell'Aquila *et al.*, Nucl. Instrum. Meth. Phys. Res. A **929**, 162 (2019).
[16] R. Palit *et al.*, Nucl. Instrum. Meth. Phys. Res. A **680**, 90 (2012).
[17] S. E. Arnell, H. Linusson, and Z. Sawa, Nucl. Phys. A **166**, 241 (1971).
[18] F. Pühlhofer, Nucl. Phys. A **280**, 267 (1977).
[19] A. V. Ignatyuk, G. N. Smirenkin, and A. S. Tishin, Sov. J. Nucl. Phys. **21**, 255 (1975).
[20] F. D. Becchetti and G. W. Greenlees, Phys. Rev. **182**, 1190 (1969).
[21] P. Moller, J. R. Nix, W. D. Myers, and W. J. Swiatecki, At. Data Nucl. Data Tables **59**, 185 (1995).
[22] I. Stefanescu *et al.*, Phys. Rev. C **79**, 064302 (2009).
[23] R. Capote *et al.*, Nucl. Data Sheets **110**, 3107 (2009).
[24] T. von Egidy and D. Bucurescu, Phys. Rev. C **80**, 054310 (2009).
[25] S. M. Grimes, T. N. Massey, and A. V. Voinov, Phys. Rev. C **99**, 064331 (2019).